J. Geomag. Geoelectr., **49**, 1451–1468, 1997

Robust Processing of Magnetotelluric Data from the Auroral Zone

Xavier GARCIA[1], Alan D. CHAVE[2], and Alan G. JONES[3]

[1] *Departament de Geologia Dinamica i Geofisica, University of Barcelona, Marti i Franques s/n, E-08028 Barcelona, Spain*
[2] *Woods Hole Oceanographic Institution, Woods Hole, MA 02543, U.S.A.*
[3] *Geological Survey of Canada, 1 Observatory Crescent, Ottawa, Ontario K1A 0Y3, Canada*

(Received November 11, 1996; Revised May 7, 1997; Accepted May 15, 1997)

Magnetotelluric (MT) data acquired during September–October, 1994, in northern Canada, were strongly influenced by non-uniform source field contributions from the auroral electrojet, and especially by intense auroral episodes. The largest effect on the estimate of the magnetotelluric impedance tensor elements was during intervals of highest magnetic activity, which primarily correlated with high auroral activity and was observed during local nighttime. In comparison, during the day the effect on the normal magnetotelluric impedance tensor response was usually, but not always, small. A robust controlled-leverage processing algorithm was applied to these data in an attempt to extract the stable uniform field estimates of the impedance. The differences between nonrobust and robust processing of the entire data set is compared to that obtained after dividing the time series into daytime and nighttime segments. The nonrobust estimate using all data is controlled by the nocturnal data, which are, in turn, dominated by non-uniform source effects. However, nonrobust processing of only the daytime data fails to recover a useful result. There is little difference between the robust response for the entire and daytime data provided that the fraction of auroral activity is not large, i.e., in excess of half of the available data series. In addition, examination of the time-dependence of the response functions shows that the strongest bias is observed during the initial quarter of an auroral event.

1. Introduction

High geomagnetic latitude magnetotelluric (MT) data are often strongly influenced by electrojet current systems flowing above the observation site. The electrojet is a complex, low altitude (100–120 km) current system whose position is strongly time dependent, but usually constrained to lie within an oval band between 58–75° geomagnetic latitude (Fig. 1), depending on the relative position of the Sun. During the day, the oval weakens in intensity and moves to higher latitudes, whereas at night the oval strengthens and descends to the south. The most intense ionospheric currents flow in the nighttime sector, causing a high level of geomagnetic activity, while during the day normal processes in the magnetosphere dominate the geomagnetic field. The most complex ionospheric current systems occur during the collision of the evening eastward electrojet and the early morning westward electrojet, and this event is known as the Harang discontinuity. Due to its close proximity to the Earth, the ionospheric currents produces short wavelength, non-plane wave source fields which violate the usual magnetotelluric plane wave (MT) assumptions, and yield a time-varying Earth response function. Figure 2 illustrates the effect of a finite single wavelength source field component (Price, 1962; Srivastava, 1965) on the apparent resistivity and phase above a one-dimensional (1D) Earth appropriate for northern Sweden (Jones, 1980). While aurorae will typically produce source fields covering a continuum of length scales rather than a single one, these will typically be dominated by wavelengths of order the horizontal scale of the ionospheric current systems, or a few hundred to perhaps as much as a thousand kilometres. Figure 2 shows that this can result in appreciable bias to the apparent resistivities and phases at

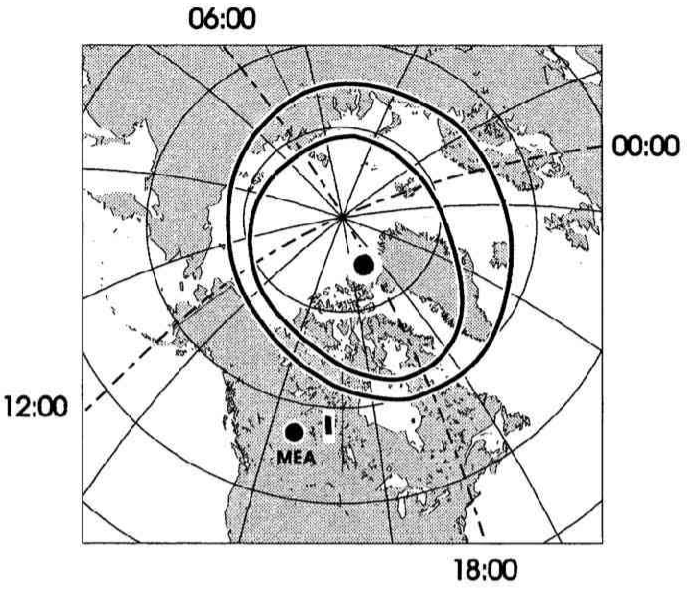

Fig. 1. The polar electrojet oval over the northern hemisphere is delineated by the solid ellipses. Four meridians showing the relative magnetic local time have been added. The thick line in northern Canada shows the position of the MT profile. The dots indicate the location of the geomagnetic North Pole and Meanook Observatory. Modified after Pettersen (1992).

periods longer than a few tens of seconds.

Due both to mathematical and interpretational difficulties, most previous work on auroral effects has been theoretical and confined to simplified source field models such as line currents. Some examples include Hibbs and Jones (1978), Mareschal (1981, 1986), Jones (1980, 1981), Jones *et al.* (1983), Kaikkonen (1986), Hermance (1984), and Osipova *et al.* (1989). Mareschal (1986) gave a particularly good review of the influence of nonuniform source fields on the MT transfer functions for a 1D earth. The source effects increase with period at a given location, but decrease with distance from the electrojet. MT measurements made at long periods directly under the electrojet tend to underestimate the resistivity and overestimate the phase, while the reverse is true past the edge of the electrojet (see references above). Since the electrojet meanders meridionally, a complex time-dependent mixture of these effects will be obtained. The energetic, highly variable nature of the auroral electrojet is analogous to that of other impulsive, non-Gaussian electromagnetic disturbances, whether natural or man-made. Significant progress has been made in dealing with these problems through various data-adaptive weighting or robust processing schemes over the past decade (e.g., Egbert and Booker, 1986; Chave *et al.*, 1987; Chave and Thomson 1989; Larsen 1989; Larsen *et al.*, 1996).

The generally superior performance of robust processing methods was documented by Jones *et al.* (1989) through comparisons of different MT processing schemes applied to the same data. The cited methods are capable of eliminating bad electric field data under broad conditions. More recently, data from a lake-bottom long period MT site in central Ontario were found to be seriously contaminated by source field effects that were, at least partially, of auroral origin (Schultz *et al.*, 1993), and led to the development of robust controlled leverage processing which eliminates contaminated data in both the electric and magnetic fields (Chave and Thomson, 1997).

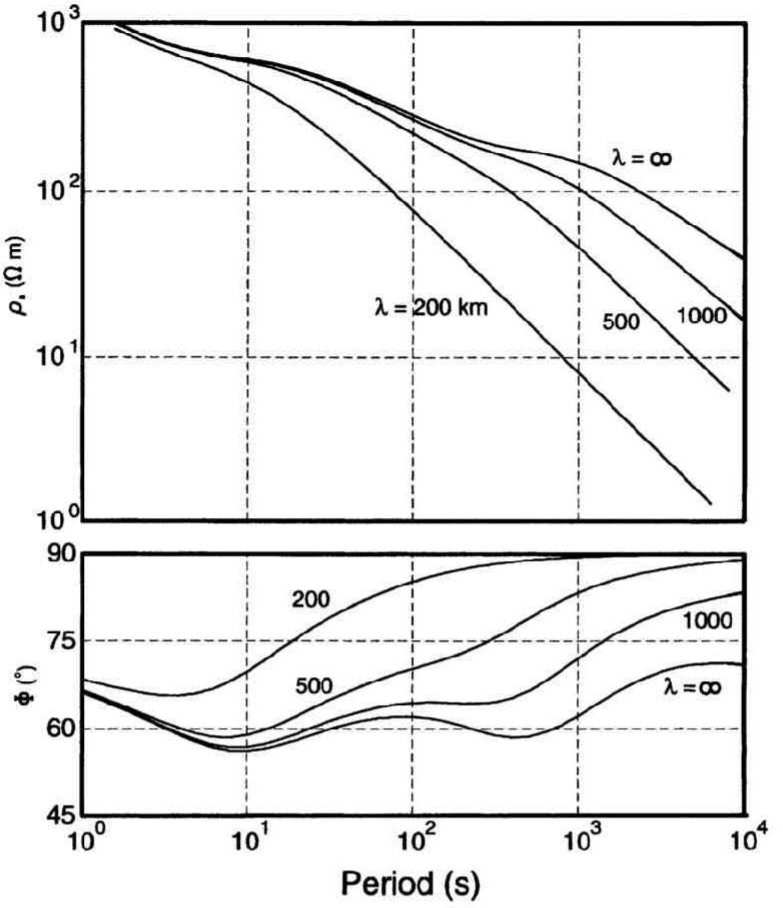

Fig. 2. The effect of a finite wavelength source field component on the apparent resistivities and phases over a model earth from Fennoscandia, taken after Jones (1980). The curve labelled ∞ represents the plane wave response. The other curves assume a single wavenumber representation of the source field with equivalent wavelengths of 1000 km, 500 km and 200 km.

Further experience with this approach is needed to assess fully its capabilities, and hence it is appropriate to test it on MT data known to be heavily contaminated by auroral effects. In the present paper, results are presented from robust controlled leverage processing of two MT stations recorded in northern Saskatchewan, Canada, which were strongly affected by the auroral electrojet. The auroral activity during acquisition was, on occasion, visible either directly overhead or even to the south, rather than being to the north as expected from the quiet time position of the auroral oval.

Defining the daytime as the interval from local 0600 to 1800, and the nighttime from local 1800 to 0600, the data have been divided so that daytime/nighttime processing can be compared to that for the entire data set. The daytime robust estimates are assumed to be a clean reference for each station. Nonrobust processing fails in all instances; even the daytime nonrobust responses differ significantly from their robust counterparts and display unphysical discontinuities in response with frequency. In contrast, the robust daytime and entire results are similar, smooth functions of frequency. However, comparison of the robust night and day/entire results reveals

significant bias in the former. Overall, this shows that a robust controlled leverage algorithm is capable of eliminating nearly all of the nighttime auroral data along with the most energetic daytime components provided that there is an adequate quantity of clean daytime data to define good values. The algorithm can fail when the noise contamination is severe (typically 40–50% of the data or more). The causes for both the nonrobust/robust and varying time segment differences are explored in both the frequency and time domains, illustrating the ability of the method to remove auroral time segments and showing that the strongest response function bias is typically observed during the first quarter of an auroral event.

2. Data

The data analysed in this study were acquired by the Geological Survey of Canada in Fall, 1994, during the Lithoprobe study of the North American Central Plains anomaly (NACP) and its relationship to the Paleoproterozoic Trans-Hudson orogen (THO) (see, e.g., Jones *et al.*, 1993). Both wideband (10 kHz to 2,000 s) and long period (5 s sampling interval) MT data were collected at each location, but only the latter are studied here. The long period data were acquired using the GSC's LiMS (Long period Magnetotelluric System) systems, which use three-component, low noise (32 pT/sqrt(Hz) at 1 Hz) ring-core magnetometers and digital recording in RAM. Sites were spaced 5–10 km apart along an approximately north-south profile extending from about 56–58° latitude near the Saskatchewan-Northwest Territories border. The profile was located directly on basement, and extended from the first arc domain in the internides of the THO, the La Ronge arc, to the Hearne bounding Archean craton. The objective of the Lithoprobe investigation was further location and definition of the NACP, which has previously been interpreted as the geophysical signature of the Proterozoic collision zone extending from the southern Rockies to northern Canada (Alabi *et al.*, 1975; Camfield and Gough, 1975; Jones *et al.*, 1993).

Data from two sites, THO400 and THO403, are analysed in this paper. The geographic and geomagnetic locations of the stations, and orientations of the x-direction relative to geographic north, are listed in Table 1.

Table 1. Geographic and Geomagnetic co-ordinates of the sites.

Station	Latitude	Longitude	Latitude	Longitude	Orientation
THO400	57°58'54"	103°47'44"	66°24'36"	315°6'0"	37°
THO403	57°34'17"	103°56'13"	65°59'24"	315°12'0"	35°

Electrojet effects are evident in the raw MT data, especially during nighttime intervals. These are manifest as strong negative excursions of the north magnetic field and increased activity in the electric fields. Figure 3 shows the total recorded time series from site THO400 together with the station K index of geomagnetic activity recorded at Meanook, the nearest observatory in the Canadian system. K indices are a quasi-logarithmic measure of geomagnetic activity (Menvielle and Berthelier, 1991). Ten class limits lie between $K = 0$ (magnetic quietness) and $K = 9$ (magnetic storm), with a lower threshold for $K = 9$ of 1500 nT for Meanook Observatory. In particular, the $K = 7$ index in the figure is equivalent to a 3 hour range of 600–989 nT, indicative of strong geomagnetic activity. The overall effect of the intense night activity of the auroral electrojet is clear in both the data and in the index.

3. Robust Controlled Leverage Response Function Estimation

Chave and Thomson (1989, 1997) describe the statistical basis and numerical implementation of the robust and robust controlled leverage algorithms used in this paper, and only a summary

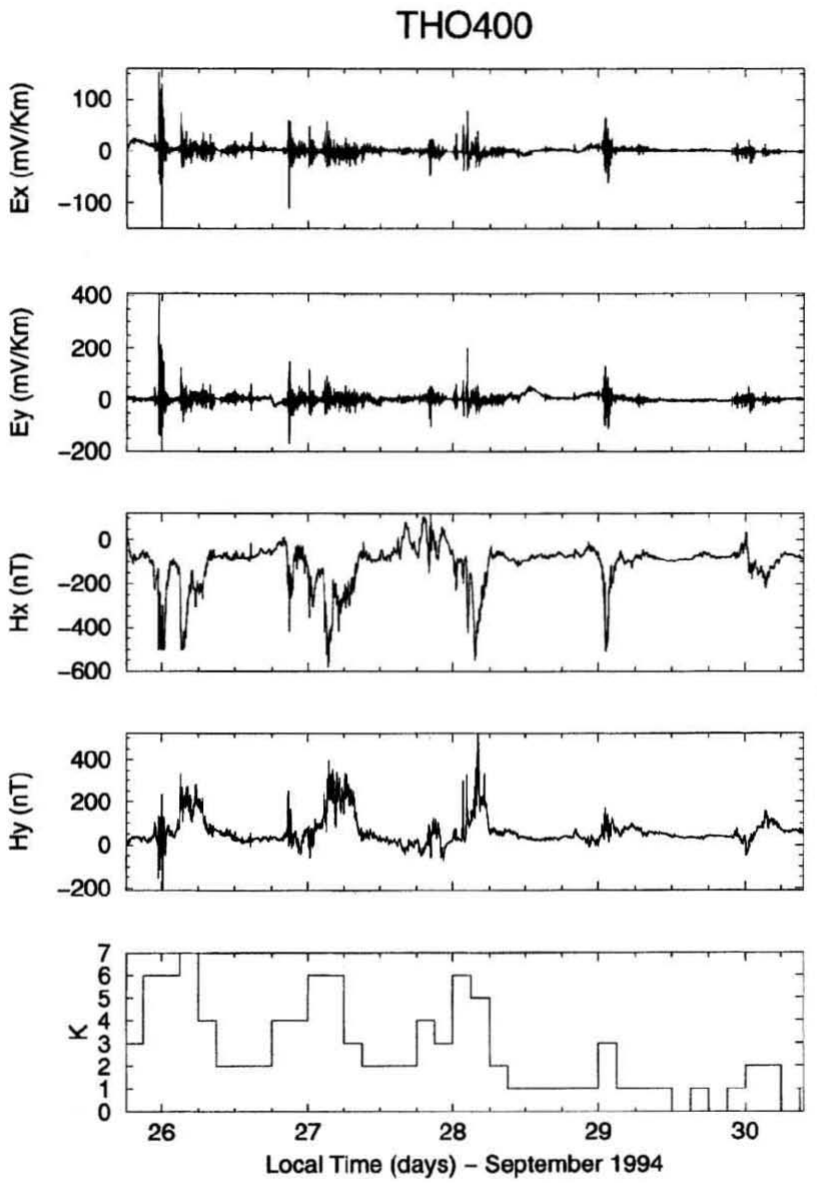

Fig. 3. The raw time series for the horizontal electric and magnetic fields at station THO400 together with the K index of magnetic activity from Meanook Observatory.

will be presented here. A general review of robust statistics may be found in Chave *et al.* (1987). In addition, the application of the nonparametric jackknife to constructing confidence limits on coherences and transfer functions is thoroughly described by Thomson and Chave (1991).

For each of the sites, the raw time series recorded at 5 s interval were re-processed using an extension of the robust method of Chave and Thomson (1989). Remote reference processing was not undertaken, but given the high sensitivity and low noise of the magnetometer, autopower noise bias is rarely a problem with the LiMS units at the periods of interest. The robust estimator

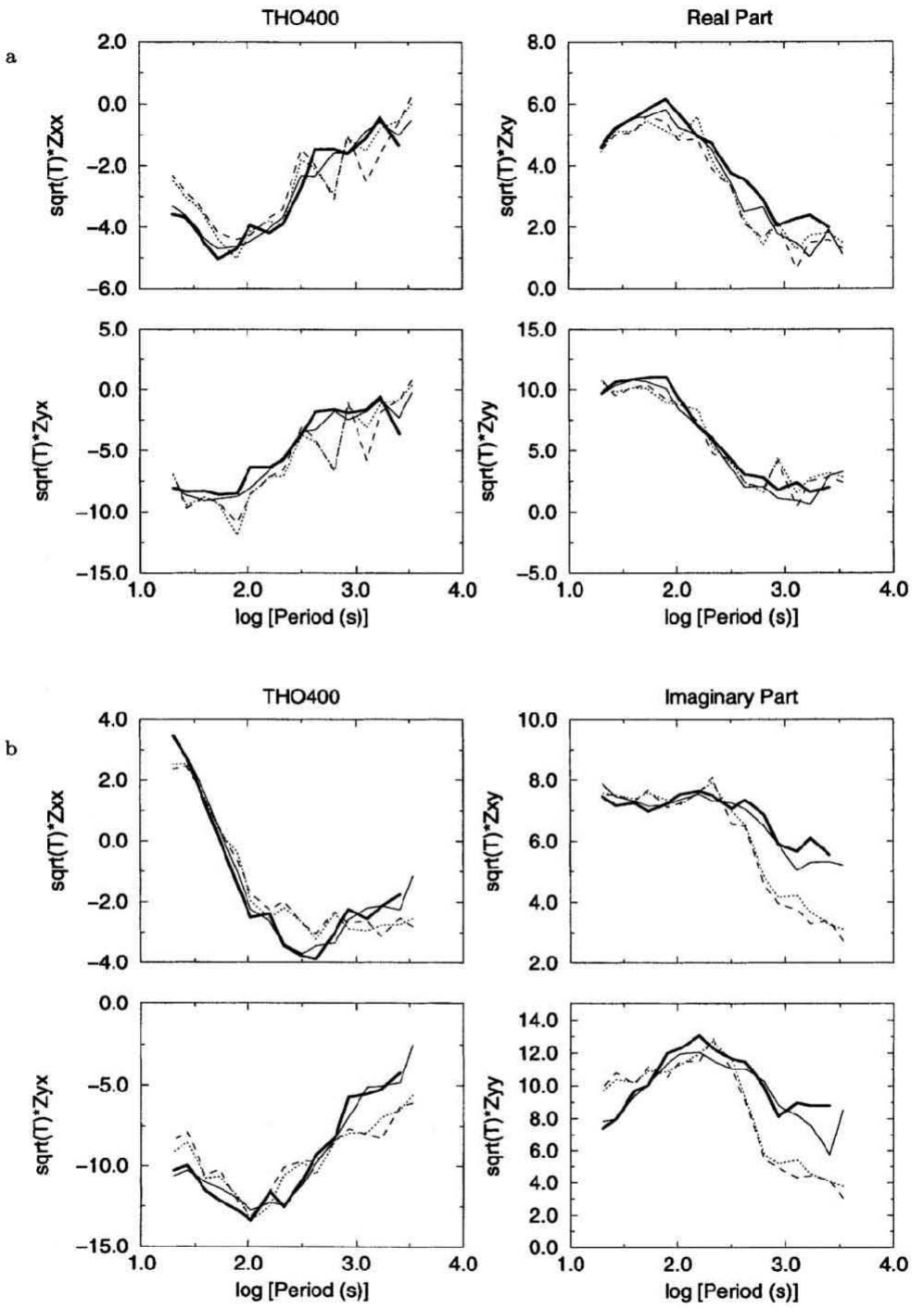

Fig. 4. The impedances scaled by the square root of period for station THO400. Figures 4a and 4b show the real and imaginary parts of the responses, respectively. For each figure, the traces are: thick line, robust estimate using the daytime data; thin line, robust estimate using all of the data; dotted line, nonrobust estimate using all of the data; dashed line, nonrobust estimate using the nighttime data. The units of the period-scaled impedance are field units by square second.

of Chave and Thomson (1989) is based on iterative re-weighting of the least squares solution for the usual MT response function relating the Fourier transforms of the horizontal electric and magnetic fields. The weights are chosen in a data-adaptive manner based on the size of the regression residuals relative to those that would be expected for Gaussian data. This approach is very effective in detecting and removing outliers in the electric field, but is not especially sensitive to anomalous magnetic field values. For this and other reasons, the approach of Chave and Thomson (1989) has been extended to incorporate:

(i) automatic use of variable section sizes such that the frequency of interest is always of order the inverse section length,

(ii) coherence thresholding of the time series prior to robust processing to eliminate noisy data segments,

(iii) nonparametric jackknife error estimates, and

(iv) a new method for automatically controlling leverage by anomalous magnetic field values in addition to robust removal of outliers in the electric field.

The use of short data sections has been shown empirically to facilitate detection of electric field outliers, especially the most common form which occur in correlated clumps (most notably in the presence of aurorae) rather than as infrequent isolated anomalous points. Coherence thresholding has previously been shown to aid in eliminating low signal-to-noise ratio intervals dominated by instrumental noise (Egbert and Livelybrooks, 1996). The statistical basis for leverage control based on the size of the hat matrix diagonal elements is described by Chave and Thomson (1997),

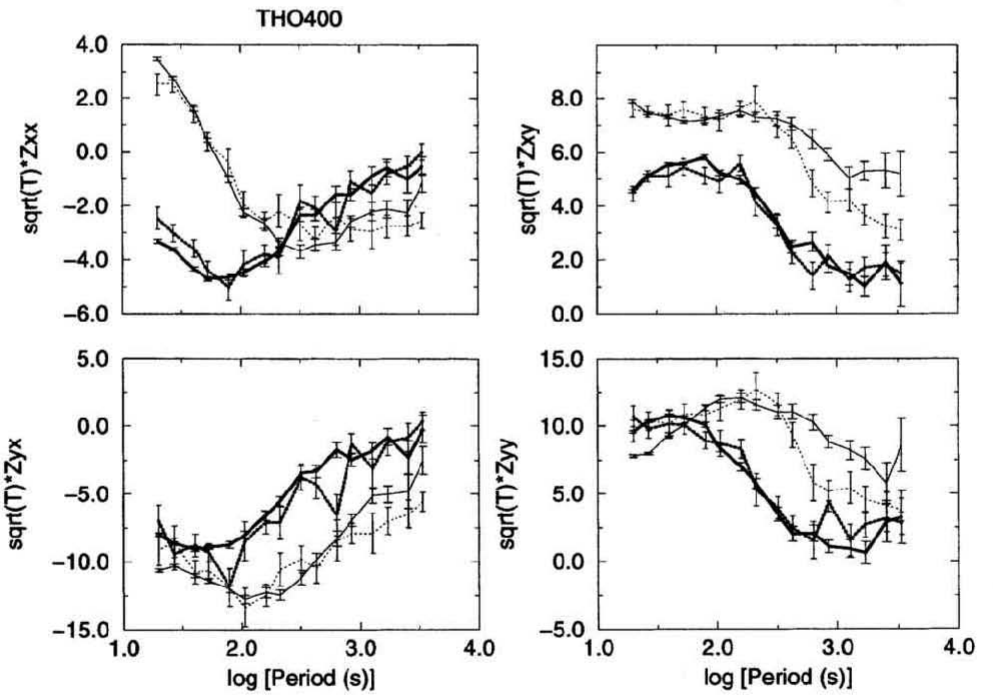

Fig. 5. The impedance at station THO400 scaled by the square root of period including the double-sided 95% confidence limits. The solid line shows the estimate from robust processing of all of the data, while the dashed line shows the estimates from nonrobust processing using all of the data. The thick and thin lines show the real and imaginary parts of the estimates, respectively. The units of the period-scaled impedance are field units by square second.

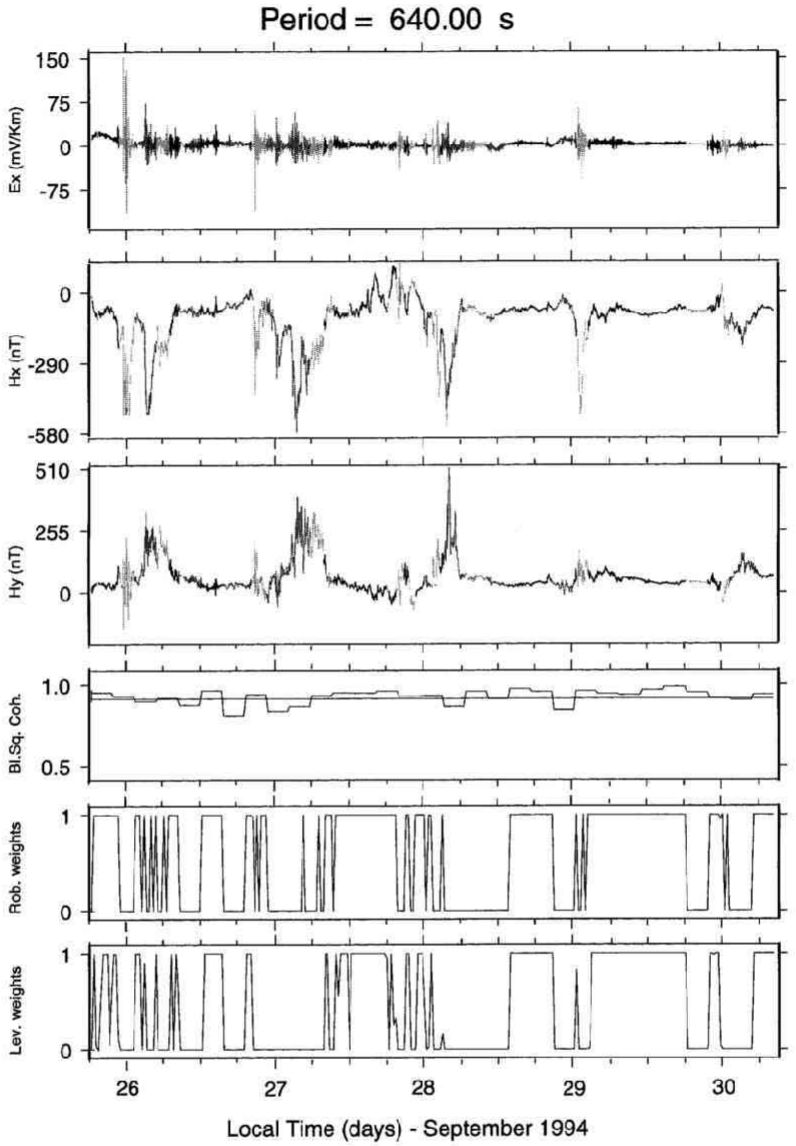

a

Fig. 6. The time series at station THO400 coded according to whether the data for the corresponding segment have been either accepted or rejected by coherence thresholding and robust controlled leverage weighting at a period of 640 s. Figures 6a and 6b show this for the E_x and E_y estimates, respectively. The top three plots in each panel show the electric and the two horizontal magnetic field time series. A black trace indicates good data, while a dark grey corresponds to data which have been eliminated by block coherence thresholding below a value of 0.912 and a light grey trace indicates data which have been eliminated by a combination of robust and controlled leverage weighting. The bottom three panels show the block squared coherence and the robust and leverage weights.

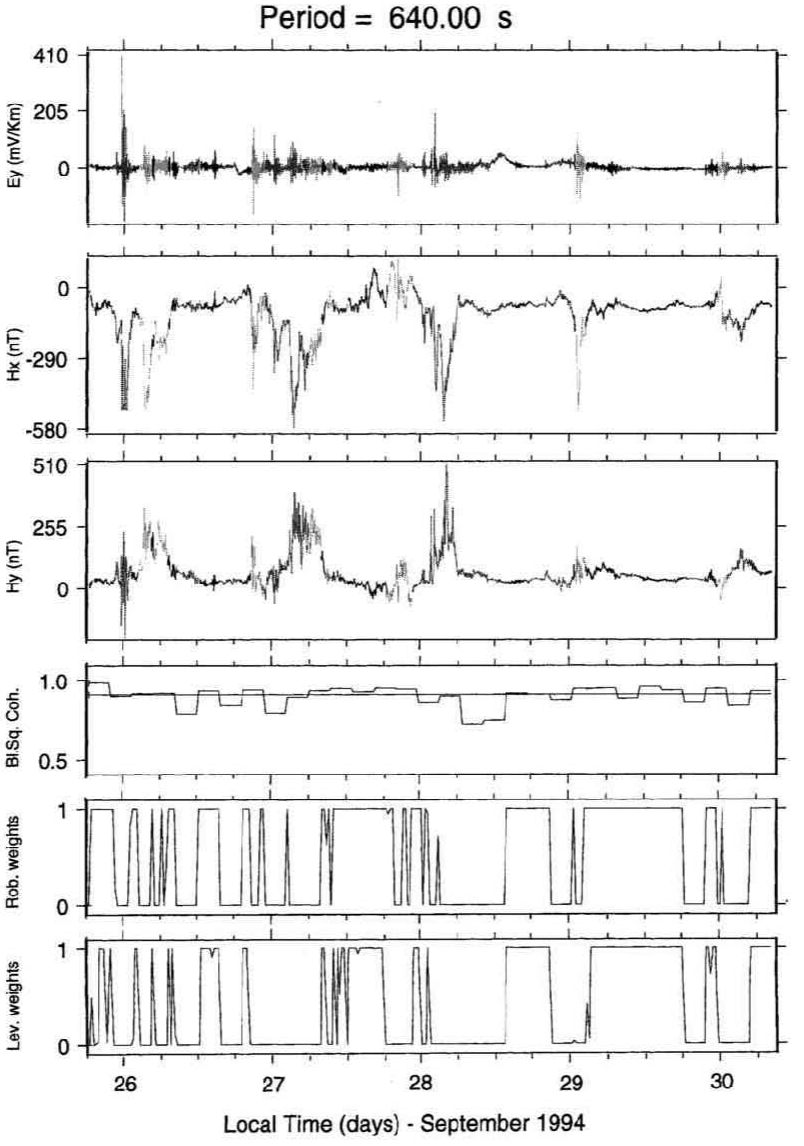

b

Fig. 6. (continued).

who also document its efficacy in dealing with data where source field problems are prevalent.

The MT response tensors for sites THO400 and THO403 were computed at periods ranging from 20 s–3,000 s, with seven estimates per decade spaced approximately equally in logarithmic range. The data were processed in the orientation in which they were collected (see Table 1), so that the x- and y-axes are approximately in the geomagnetic north and east directions, respectively.

4. Analysis

4.1 Site THO400

Figures 4a and 4b compare the real and imaginary parts of the MT impedance estimates (scaled by the square root of period for clarity in this and subsequent figures), respectively, for robust processing of the entire and daytime series and nonrobust processing of the entire and nighttime data. Robust processing of the daytime data serves as a clean reference for the MT response due to the relative minimum in auroral activity. Nonrobust processing of the entire data set yields results that are comparable to those from the nighttime data. The latter are expected to be strongly biased by the aurora, and it is clear that nonrobust processing of the entire data set is dominated by the energetic nighttime interval, as is usual with conventional least squares estimators. This is especially apparent in the imaginary part of those responses involving H_y (i.e., Z_{xy} and Z_{yy}) at long periods, and in the unphysical kinks in the responses as a function of period. In contrast, robust processing of the entire data set yields results which are similar to those from the daytime data, and hence the robust controlled leverage estimator is capable of discriminating and eliminating most of the energetic auroral intervals. However, robust processing is somewhat more effective at detecting and rejecting auroral effects at short periods, as reflected in the relative scatter seen in Fig. 4. This is because the early morning (0600–0900) or late afternoon (1500–1800) intervals may be affected by the aurora to varying degrees, and the longer data sections required at long periods may be contaminated to some extent. This is less of a problem for the daytime robust data processing because bad data constitute a very small fraction of the total, whereas the entire time series contains more unusual values. Finally, Fig. 4 shows that use of a robust algorithm for processing MT data from the auroral zone gives vastly superior results, and indicates that, at least for some stations and some intervals, no manual editing of the time series (such as separation into day and night intervals) is necessary to obtain good estimates.

A more detailed comparison of the robust and nonrobust estimates for all of the data, including double-sided 95% jackknife confidence limits, is shown in Fig. 5. It is clear that robust processing yields generally smoother estimates. This is especially apparent at long periods, where the nonrobust result displays frequent and unacceptable kinks. Note also the difference in the size of the error bars; the jackknife gives smaller confidence limits for the robust estimates because the residuals are more homoscedastic and approximately Gaussian, in contrast to the more heteroscedastic nonrobust residuals. The differences between the robust and nonrobust responses are typically significant at the 95% level at long periods, but are in better agreement at short periods. This observation also holds for the results shown in Fig. 4 because the robust confidence limits are approximately the same for the day and entire data processing since they employ nearly the same data segments after weighting. The nonrobust confidence limits for the nighttime and entire data sets are also comparable in size (but larger than their robust counterparts) because both types of processing are dominated by the energetic auroral-contaminated nighttime segments. Similarly, nonrobust processing of the daytime data also shows more scatter outside of the 95% confidence band. In fact, some estimates lie almost 10 standard errors away from the daytime robust values, and hence the differences are significant at a very high statistical level.

Figure 6 displays the total recorded time series coded to show those sections used in the final estimate of the impedances and those rejected by the algorithm (either through coherence thresholding or by robust and/or controlled leverage weighting) for a period of 640 s. The coherence threshold for this period was 0.912. These plots demonstrate that the algorithm systematically downweights the more energetic auroral sections which occur principally during the nighttime, and retains most of the daytime sections for the final estimate. These plots also show the block coherence estimate used for thresholding and the robust and leverage weights. The former does eliminate a limited part of the auroral intervals (often due to instrumental problems like clipping

when the field strength is greater than the sensor dynamic range) but is not effective at removing most of them because they remain highly coherent in the presence of non-uniform source fields. The robust and controlled leverage weights are much more effective in the role of removing anomalous source effects. A comparison of the robust and leverage weights shows the importance of the latter in downweighting some sections not discarded by the robust weights, and underscores the inability of robust weights alone to detect anomalous data in the magnetic field.

Figure 7 shows nonrobust estimates of the impedance as a function of time. The data have been split into sections of length 1024 points and the nonrobust response was estimated for a period of 106.6 s using a modified form of Wight and Bostick's (1980) cascade decimation scheme (method 4 in Jones *et al.*, 1989). The time-dependent response is then plotted together with the raw time series for the principal magnetic field component. The double-sided 95% confidence bound on the robust estimate using all of the data is also depicted as two horizontal lines. Note that the strongest bias in the nonrobust estimate is typically observed at the leading edge of a

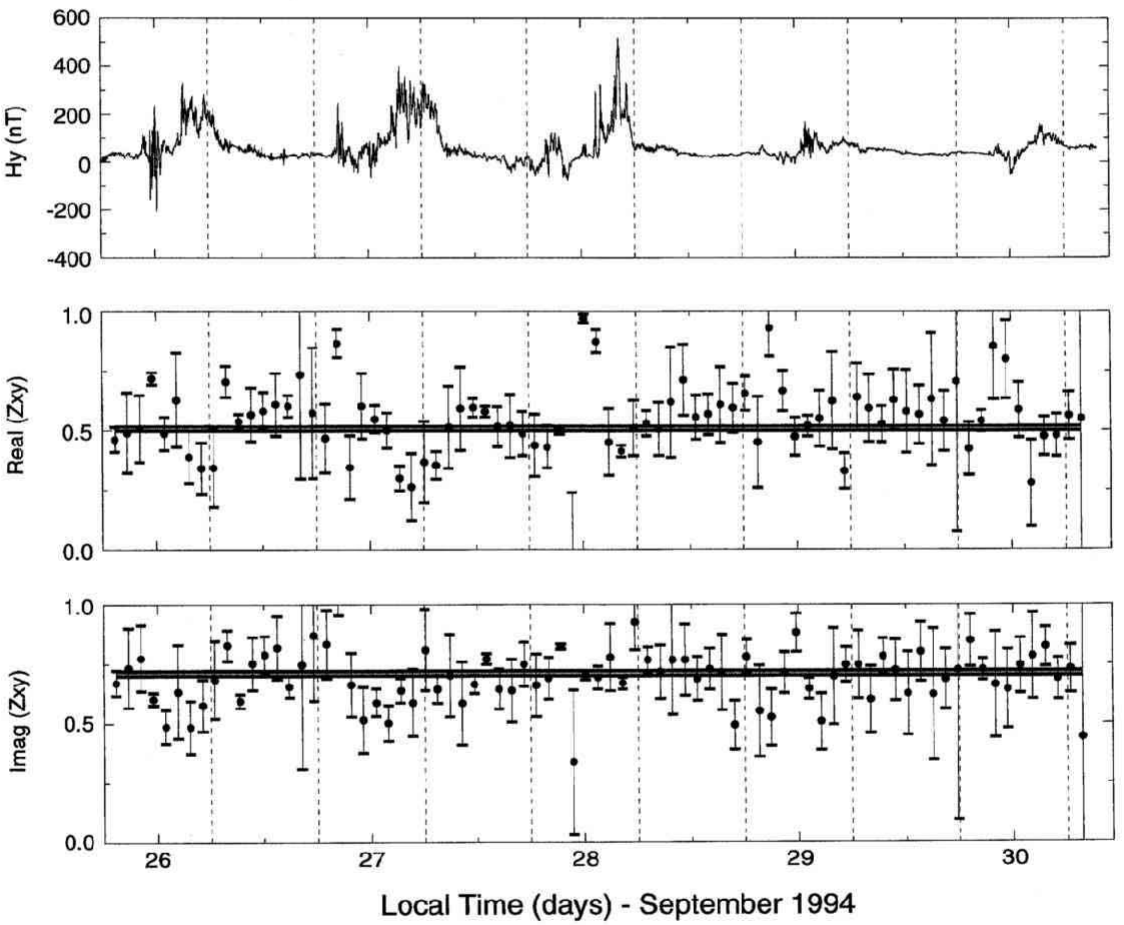

Fig. 7. Temporal variation of nonrobust estimates of the impedance tensor component Z_{xy} MT response obtained using adjacent sections of 1024 data points at a period of 106.6 s. The responses are placed under the corresponding magnetic field data (H_y). The 95% confidence bounds of the robust estimate using all of the data are depicted by two horizontal lines. Impedance in field units.

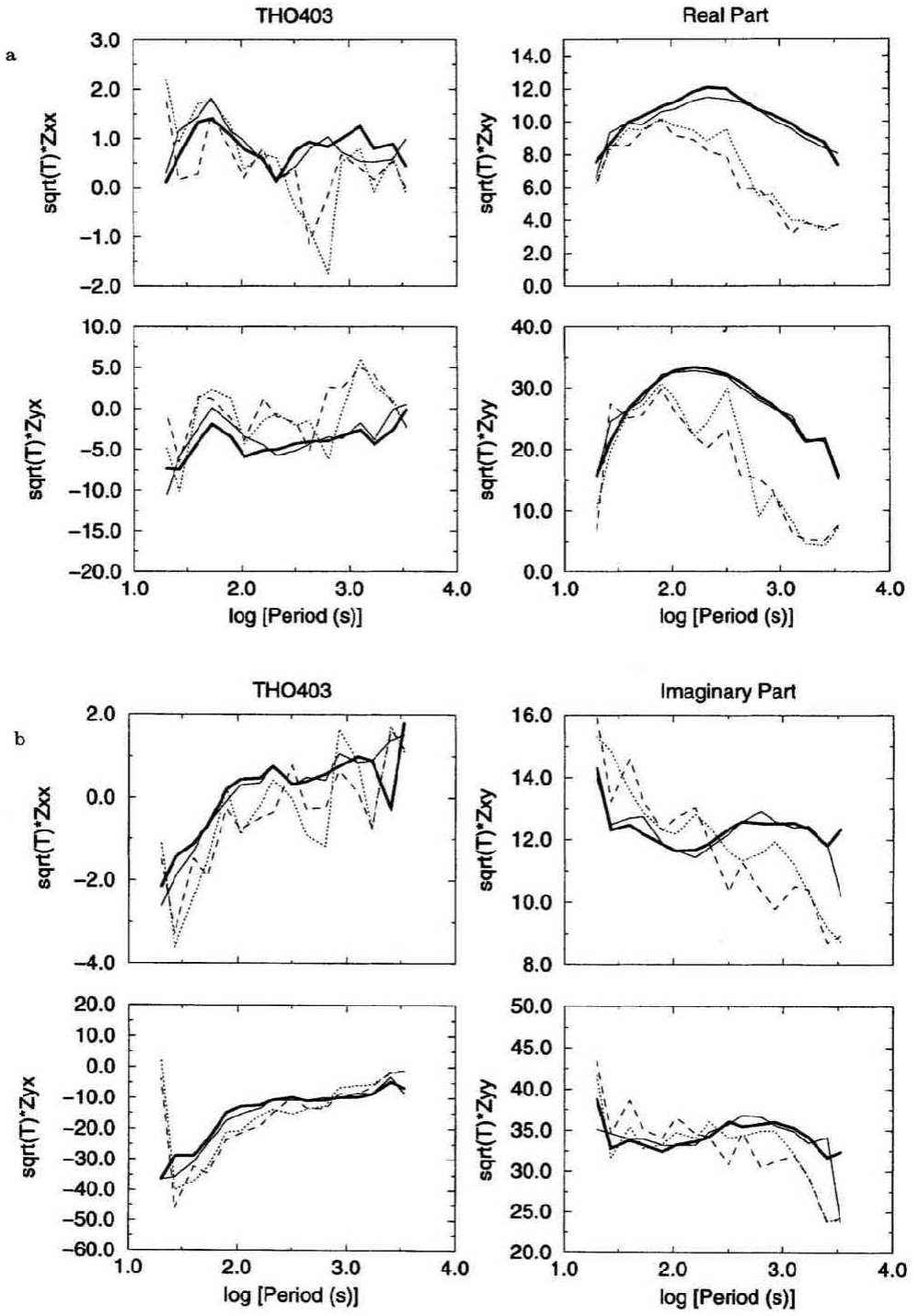

Fig. 8. Same as Fig. 4 for station THO403.

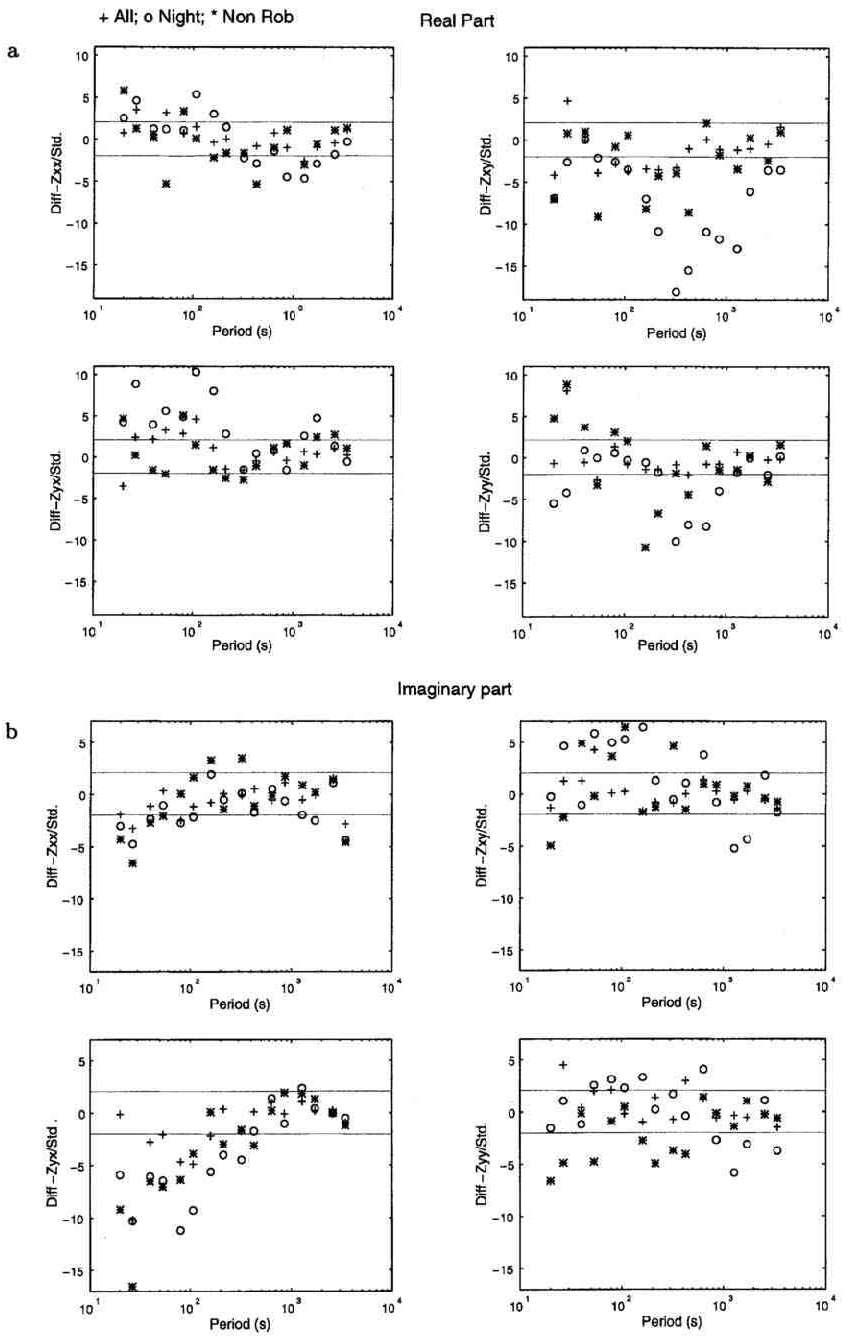

Fig. 9. Standardized (Studentized) differences of the robust estimates at station THO403 using robust estimates of the daytime data as a reference. Figures 9a and 9b show the real and imaginary parts, respectively. The plotted statistic is the difference between a given estimate and the robust daytime estimate divided by the jackknife standard error of the daytime robust estimate, and shows graphically when a given estimate varies at a given significance level from the reference value. The symbols are: +, standardized differences for robust processing of all the data; o, standardized differences for robust processing of the night data; *, standardized differences for nonrobust processing of the daytime data. The two horizontal lines show the double-sided 95% confidence band.

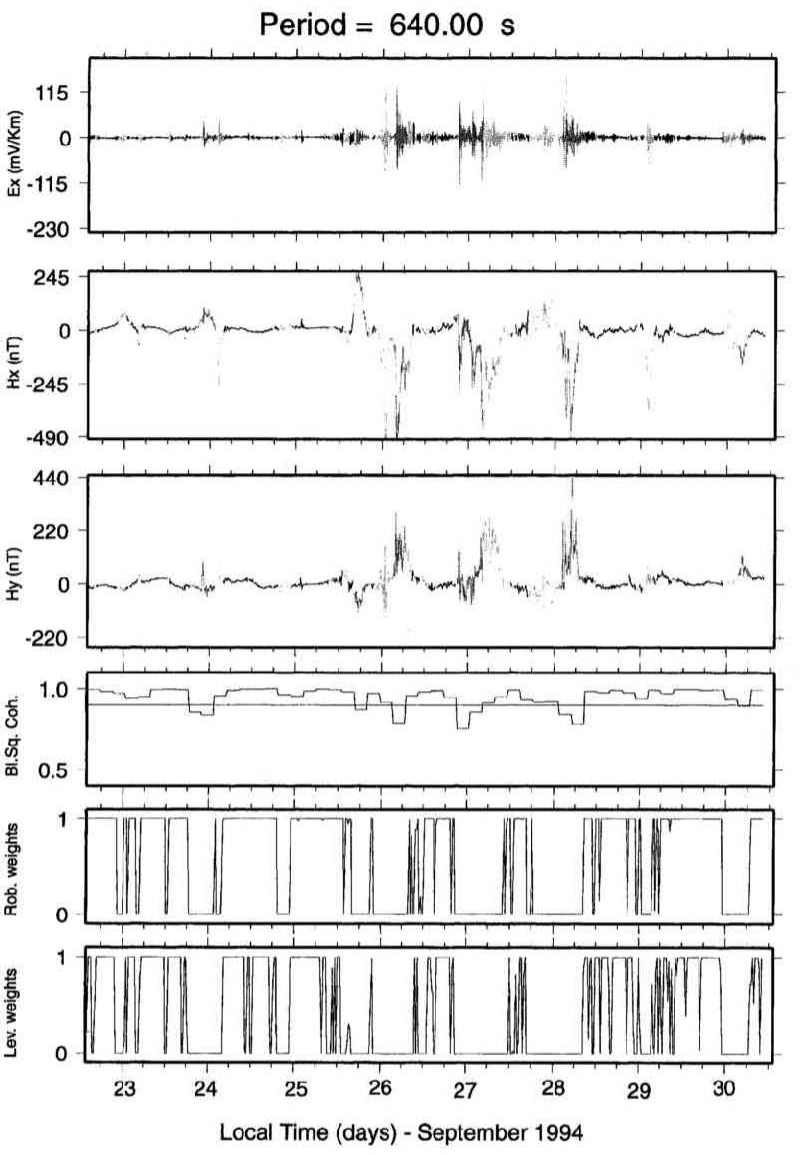

a

Fig. 10. Same as Fig. 6 for station THO403, the block coherence thresholding for this station is 0.900.

nighttime auroral event, with overestimates of the impedances. Most of the nonrobust responses are biased relative to the robust estimate, and underscores the manner in which nonrobust methods failed in all cases, including using all of the daytime data. The erratic behaviour of the nonrobust estimate is due to temporal variability in the location and intensity of the electrojet, and cannot be explained by unsophisticated source models. In particular, note that contrary to the predictions from oversimplified source field models which always yield underestimates of the correct response in the presence of electrojets (e.g., Price, 1962; Osipova *et al.*, 1989), the

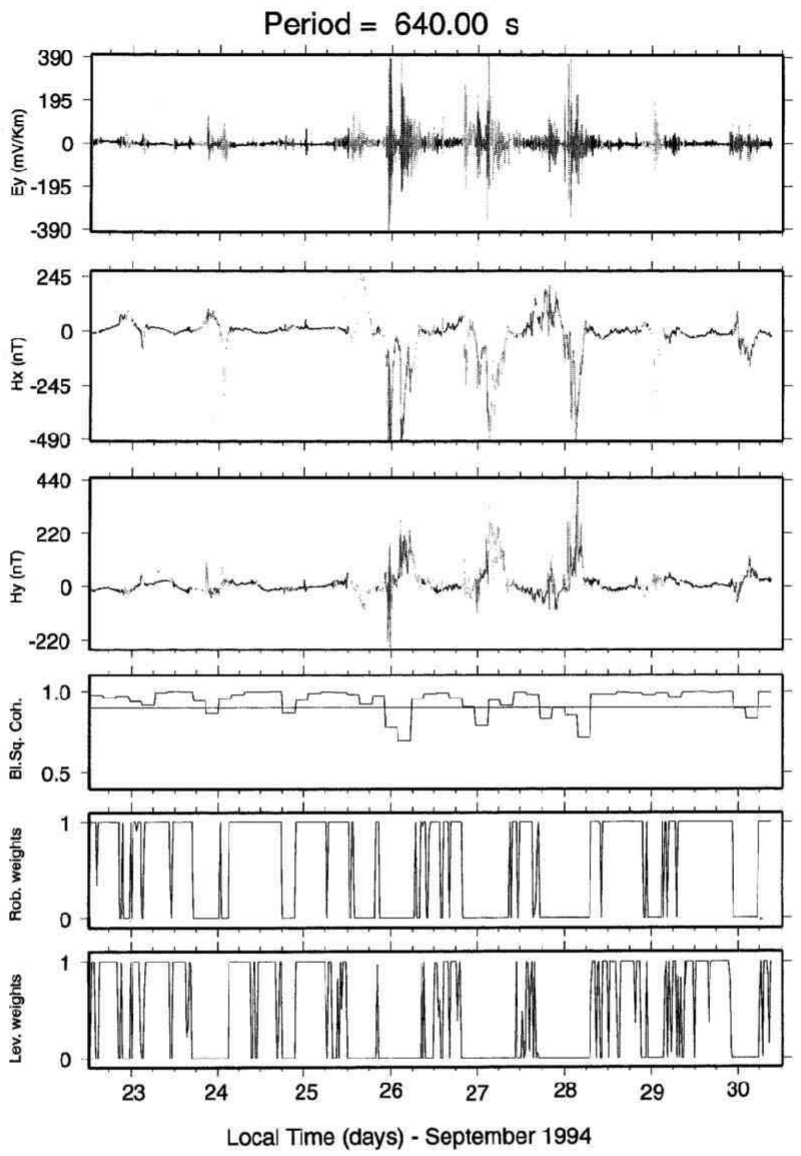

b

Fig. 10. (continued).

effect of ionospheric and magnetospheric activity is, in reality, both complex and unpredictable. For example, the onsets of substorm are always accompanied by overestimates in the response functions.

4.2 Site THO403

Results from processing station 403 are shown to demonstrate that robust methods can fail in the presence of a large amount of contaminated data. This should not to be surprising; robust

methods operate by detecting values which are anomalous relative to the bulk of the sample, and are inherently incapable of detecting contaminated data which exceed half of the total sample. In cases like this, it is necessary to edit the time series manually prior to robust processing so that the time series will be less extensively affected from the start. The response functions corresponding to robust processing of the entire and daytime data set and nonrobust processing of the entire and nighttime data set, analogous to Fig. 4 for station THO400, are plotted in Fig. 8. Note the effect of the aurora on the nonrobust responses which are badly biased relative to the robust daytime results at periods over a few tens of seconds. As with THO400, it is clear that the nighttime auroral intervals dominate the result when the entire data set is processed. Robust processing corrects this and appears to drive the result for the entire data set towards that for the uncontaminated daytime interval. In fact, the improvement from robust processing is profound at first glance, and appears to be more extensive than for THO400; this is especially evident in the smoothness of the robust Z_{xy} and Z_{yy} responses relative to their nonrobust counterparts.

However, the standardized differences shown in Fig. 9 portray a somewhat different story. The differences between the robust results for the entire and daytime data are significant at many more periods than expected for Gaussian data. This is more apparent for station THO403 than for THO400 because the error estimates are notably smaller for this site, and hence smaller differences have greater significance. For many periods the difference between the entire and daytime robust estimates is larger than 5 standard errors, suggesting that this station is more strongly affected by the aurora. For the robust estimates of the nighttime data, the differences are also bigger for this station. One possible reason for the differences in behaviour between the two stations is the difference in the local geological structure which results in the MT impedance tensor for station THO403 containing more significant amplitudes in the diagonal estimates compared to station THO400. The combination of 3D source effects and 3D distorting or geological structures may be the reason for the robust processing failure for station THO403.

Figure 10 shows the time series at station THO403 coded to show those sections which are rejected by either coherence thresholding or robust weighting at a period of 640 s, as for THO400 in Fig. 6. The robust weighting rejects mainly the energetic night sections, but also affects the day data in some instances. Note that for 27 September only daytime data around local midday have been accepted, and large amounts of daytime data have been rejected. Comparison of Figs. 6 and 10 shows that the electric field data from station THO403 is much more strongly influenced by the aurora, and hence the robust algorithm has a more difficult time distinguishing normal from anomalous intervals.

5. Conclusions

From processing data from two sites that are heavily influenced by auroral effects, four conclusions can be drawn:

· The effects of nonuniform sources can strongly bias the response tensor and hence distort geological interpretations unless measures are taken to eliminate its effects. As shown in this paper, a robust processing method can deal with bias from non-uniform source fields provided that data contaminated by source field effects do not dominate the sample.

· Nonrobust processing of data from the auroral zone fails to remove intervals that are obviously contaminated by source field effects even after data editing.

· Robust procedures need a reasonable ratio of contaminated/uncontaminated data (typically 40–50% or less) to yield reliable results. However, in the presence of a large amount of contaminated data, robust procedures can still succeed with assistance from data editing to remove the most obviously contaminated intervals.

· Although our examination of the effects of source fields on the magnetotelluric responses has only been precursory, we can conclude that the effects of time-varying ionospheric and mag-

netospheric sources on the MT responses is both complex and unpredictable.

This work was supported at WHOI by the Office of Basic Energy Sciences, US Department of Energy. This work was undertaken whilst XG was a visiting scientist at Woods Hole and the Geological Survey of Canada, and was supported by a research grant from the Spanish Science Ministry through project PB92-808. This is Woods Hole Oceanographic Institution contribution 9444, Geological Survey of Canada contribution number 1997062, and Lithoprobe publication number 872.

REFERENCES

Alabi, A. O., P. A. Camfield, and D. I. Gough, The North American Central Plains anomaly, *Geophys. J. Royal Astron. Soc.*, **43**, 815–834, 1975.

Camfield, P. A. and D. I. Gough, Anomalies in daily variation magnetic fields and structure under north-western United States and south-western Canada, *Geophys. J. Royal Astron. Soc.*, **41**, 193–218, 1975.

Chave, A. D. and D. J. Thomson, Some comments on magnetotelluric response function estimation, *J. Geophys. Res.*, **94**, 14,215–14,225, 1989.

Chave, A. D. and D. J. Thomson, On robust magnetotelluric response function estimation, *J. Geophys. Res.*, 1997 (to be submitted).

Chave, A. D., D. J. Thomson, and M. E. Ander, On the robust estimation of power spectra, coherences, and transfer functions, *J. Geophys. Res.*, **92**, 633–648, 1987.

Egbert, G. D. and J. R. Booker, Robust estimation of geomagnetic transfer functions, *Geophys. J. Royal Astron. Soc.*, **87**, 173–194, 1986.

Egbert, G. D. and D. W. Livelybrooks, Single station magnetotelluric impedance estimation: coherence weighting and the regression M-estimate, *Geophys.*, **61**, 964–970, 1996.

Hermance, J. F., Electromagnetic induction by finite wavenumber source fields in 2-D lateral heterogeneities: The transverse electric mode, *Geophys. J. Royal Astron. Soc.*, **78**, 159–179, 1984.

Hibbs, R. D. and F. W. Jones, The calculation of perturbation and induction arrows for a three-dimensional conductivity model and various two-dimensional source fields, *J. Geophys. Res.*, **83**, 5479–5485, 1978.

Jones, A. G., Geomagnetic induction studies in Scandinavia—I. Determination of the inductive response function from the magnetometer data, *J. Geophys.*, **48**, 181–194, 1980.

Jones, A. G., Geomagnetic induction studies in Scandinavia—II. Geomagnetic depth sounding, induction vectors and coast effect, *J. Geophys.*, **50**, 23–36, 1981.

Jones, A. G., B. Olafsdottir, and J. Tiikkainen, Geomagnetic induction studies in Scandinavia—III. Magnetotelluric observations, *J. Geophys.*, **54**, 35–50, 1983.

Jones, A. G., A. D. Chave, G. Egbert, D. Auld, and K. Bahr, A comparison of techniques for magnetotelluric response function estimation, *J. Geophys. Res.*, **94**, 14,201–14,213, 1989.

Jones, A. G., J. A. Craven, G. A. McNeice, I. J. Ferguson, T. Boyce, C. Farquharson, and R. G. Ellis, The North American Central Plains conductivity anomaly within the Trans-Hudson orogen in northern Saskatchewan, *Geology*, **21**, 1027–1030, 1993.

Kaikkonen, P., Numerical electromagnetic modeling including studies of characteristic dimensions: A review, *Surv. Geophys.*, **8**, 301–337, 1986.

Larsen, J. C., Transfer functions: smooth robust estimates by least-squares and remote reference methods, *Geophys. J. Int.*, **99**, 645–663, 1989.

Larsen, J. C., R. L. Mackie, A. Manzella, A. Fiordelisi, and S. Rieven, Robust smooth magnetotelluric transfer functions, *Geophys. J. Int.*, **124**, 801–819, 1996.

Mareschal, M., Source effects and the interpretation of geomagnetic sounding data at sub-auroral latitudes, *Geophys. J. Royal Astron. Soc.*, **67**, 125–136, 1981.

Mareschal, M., Modelling of natural sources of magnetospheric origin in the interpretation of regional induction studies: a review, *Surv. Geophys.*, **8**, 261–300, 1986.

Menvielle, M. and A. Berthelier, The K-derived planetary indices: description and availability, *Rev. Geophys.*, **29**, 415–432, 1991.

Osipova, I. L., S.-E. Hjelt, and L. L. Vanyan, Source field problems in northern parts of the Baltic shield, *Phys. Earth Planet. Int.*, **53**, 337–342, 1989.

Pettersen, F., Aurora borealis—the northern lights, *Way North: Earth Science, publication from Tromsø Museum, University of Tromsø*, **1**, 1992.

Price, A. T., The theory of magnetotelluric fields when the source field is considered, *J. Geophys. Res.*, **67**, 1907–1918, 1962.

Schultz, A., R. D. Kurtz, A. D. Chave, and A. G. Jones, Conductivity discontinuities in the upper mantle beneath a stable craton, *Geophys. Res. Lett.*, **20**, 2941–2944, 1993.

Srivastava, S. P., Method of interpretation of magneto-telluric data when source field is considered, *J. Geophys.*

Res., **70**, 945–954, 1965.

Thomson, D. J. and A. D. Chave, Jackknifed error estimates for spectra, coherences, and transfer functions, in *Advances in Spectrum Analysis and Array Processing, Vol. 1*, edited by S. Haykin, pp. 58–113, Prentice-Hall, Englewood Cliffs, NJ, 1991.

Vozoff, K., ed., *Magnetotelluric Methods*, Soc. Expl. Geophys. Reprint Ser. No. 5, Publ. by Soc. Expl. Geophys., Tulsa, Oklahoma, ISBN 0-931830-36-2, 1986.

Wight, D. E. and F. X. Bostick, Cascade decimation—a technique for real time estimation of power spectra, Contributed paper at Proc. IEEE Intl. Conf. on Acoust., Speech, Signal Proc., 626–629, held in Denver, CO, on April 9–11, 1980. Reprinted in Vozoff (1986).